

Classifying hydrogen-rich superconductors

E. F. Talantsev^{1,2}

¹M.N. Miheev Institute of Metal Physics, Ural Branch, Russian Academy of Sciences,
18, S. Kovalevskoy St., Ekaterinburg, 620108, Russia

²NANOTECH Centre, Ural Federal University, 19 Mira St., Ekaterinburg, 620002,
Russia

E-mail: evgeny.talantsev@imp.uran.ru

Abstract

The era of near-room-temperature superconductivity started after experimental discovery by Drozdov *et al* (2015 *Nature* **525** 73) who found that compressed H₃S exhibits superconducting transition at $T_c = 203$ K. To date, the record near-room-temperature superconductivity stands with another hydrogen-rich highly compressed compound, LaH₁₀ (Somayazulu *et al* 2019 *Phys. Rev. Lett.* **122** 027001), which has critical temperature of $T_c > 240$ K. In this paper, we analyse available upper critical field, $B_{c2}(T)$, data for LaH₁₀ (Drozdov *et al* 2019 *Nature* **569** 528) and report that this compound in all considered scenarios has the ratio of T_c to the Fermi temperature, T_F , $0.009 < T_c/T_F < 0.038$, which is typical range for unconventional superconductors. In attempt to extend our finding, we examined experimental $B_{c2}(T)$ data for superconductors in the palladium-hydrogen (PdH_x) and thorium-hydrogen-deuterium (ThH-ThD) systems and surprisingly find that superconductors in both these systems also fall into unconventional superconductors band. Taking in account that H₃S has the ratio of $0.012 < T_c/T_F < 0.039$ (Talantsev 2019 *Mod. Phys. Lett. B* **33** 1950195) we come to conclusion that in the Uemura plot all discovered to date hydrogen-rich superconductors, i.e. Th₄H₁₅-Th₄D₁₅, PdH_x, H₃S and LaH₁₀ (in this list we do not include NbTiH_x, PtH_x, SiH₄, and PH₃ for which experimental data beyond T_c are unknown), lie in same band as all unconventional superconductors, particularly heavy

fermions, fullerenes, pnictides, and cuprates, and former should be classified as a new class of unconventional superconductors.

I. Introduction

The discovery of superconductivity in highly compressed H₃S with $T_c = 203$ K by Drozdov *et al* [1] is the most fascinating breakthrough in superconductivity since epochal discovery of high-temperature superconductivity in cuprates by Bednoltz and Mueller [2]. Historical aspects of the problem can be found elsewhere [3-6].

Despite a fact that H₃S is widely classified as conventional [7] electron-phonon superconductor [1,3-6,8-13], we performed [14] analysis of experimental upper critical field data, $B_{c2}(T)$, reported by Mozaffari *et al* [15,16], and showed that H₃S is unconventional superconductor which lies in common unconventional superconductors trend band of the Uemura plot [17,18] together with other unconventional superconductors, i.e. heavy fermions, fullerenes, pnictides, and cuprates.

The concept of Uemura plot [18] is to represent all 32 classes of superconductors [19] by using two fundamental temperatures: one is the superconducting transition temperature, T_c (usually, this is used as Y-axis), and another is the Fermi temperature, T_F (usually, this is used as X-axis) [18]. In this representation all known unconventional superconductors fill a narrow band of $10^{-2} < T_c/T_F < 5 \cdot 10^{-2}$, while BCS electron-phonon mediated superconductors are located in the area of $T_c/T_F < 4 \cdot 10^{-4}$. We showed [14] that H₃S compressed at $P = 150$ GPa and 155 GPa has T_c/T_F ratio in the interval of $1.2 \cdot 10^{-2} < T_c/T_F < 3.9 \cdot 10^{-2}$, and, thus, based on general approach of Uemura *et al* [17,18], H₃S should be classified as unconventional superconductor.

Recently, further step towards room-temperature superconductivity was made by Somayazulu *et al* [20] who discovered near-room-temperature superconductivity in another

highly-compressed hydrogen-rich compound of LaH₁₀. The latter exhibits transition temperature of $T_c \gtrsim 240\text{ K}$ at external pressure in the range of $P = 150\text{-}200\text{ GPa}$ [20,21].

Drozdov *et al* [21] reported experimental upper critical field data for LaH₁₀ which we analyse in this paper and find that in all considered scenarios this compound has the ratio of superconducting energy gap, $\Delta(0)$, to the Fermi energy, ε_F , of $0.02 < \Delta(0)/\varepsilon_F < 0.07$, with respective ratio of T_c to the Fermi temperature, T_F , $0.009 < T_c/T_F < 0.038$. As the result, in Uemura plot LaH₁₀ lies in the same band as all unconventional superconductors and falls just above another hydrogen-rich counterpart of H₃S [14].

To prove that our findings in regard of H₃S and LaH₁₀ are generic features of hydrogen-rich superconductors we re-examine the upper critical field data for the first discovered superhydride superconductor Th₄H₁₅ (by Satterthwaite and Toepke [22] in 1970), and, perhaps, the most experimentally studied to date hydrogen-rich superconductors in palladium-hydrogen-deuterium system, PdH-PdD, discovered by Skoskiewicz [23] and show that despite a fact that thorium-hydrogen-deuterium and palladium-hydrogen compounds have $T_c < 8.5\text{ K}$, these low-temperature superconductors have similar ratios of $\Delta(0)/\varepsilon_F$ and T_c/T_F as ones of its near-room-temperature superconducting counterparts.

We should note that the silane, SiH₄, was the first discovered by Eremets group highly-compressed hydrogen-rich superconductor with $T_c = 17\text{ K}$ (observed at pressure of $P = 96\text{-}120\text{ GPa}$) [24]. Covalent hydride phosphine, PH₃, is another hydrogen-rich superconductor in which superconductivity with $T_c \simeq 100\text{ K}$ was discovered at $P \gtrsim 200\text{ GPa}$ [25]. And recently, superconductivity in PtH_x ($x \cong 1$) was discovered experimentally at $P = 30\text{ GPa}$ [26]. NbTiH_x [27] is another hydrogen-rich superconductor which can be potentially considered. Unfortunately, for all of these compounds, fundamental experimental data beyond T_c are unknown, and, thus, we were not able to analyse these materials in our consideration herein.

In result, we show that all discovered to date hydrogen-rich superconductors for which experimental data beyond T_c are available, i.e. Th₄H₁₅-Th₄D₁₅, PdH_x, H₃S and LaH₁₀, lie in the same band in the Uemura plot as all unconventional superconductors (particularly heavy fermions, fullerenes, pnictides, and cuprates) and thus, these superconductors should be classified as a new family of unconventional superconductors.

II. The upper critical field models

Ground state upper critical field, $B_{c2}(0)$, in the Ginzburg-Landau theory [28] is given by:

$$B_{c2}\left(\frac{T}{T_c} = 0\right) = \frac{\phi_0}{2\pi\cdot\xi^2(0)}, \quad (1)$$

where $\phi_0 = 2.068 \cdot 10^{-15}$ Wb is magnetic flux quantum, and $\xi(0)$ is the ground state coherence length. For the temperature dependent upper critical field data one of the most rigours model was proposed by Werthamer, Helfand, and Hohenberg (WHH) [29,30]:

$$\ln\left(\frac{T}{T_c(B=0)}\right) = \psi\left(\frac{1}{2}\right) - \psi\left(\frac{1}{2} + \frac{\hbar\cdot D\cdot B_{c2}(T)}{2\cdot\phi_0\cdot k_B\cdot T}\right) \quad (2)$$

where ψ is digamma function, D is the diffusion constant of the normal conducting electrons/holes. However, application of this model for the analysis of experimental $B_{c2}(T)$ data requires very often and uniformly measured dataset which covers the whole temperature range of $0 < T < T_c$ with approximate step of $(0.02 - 0.05) \cdot T_c$ between data points. In real world experiments, this condition is usually impossible to achieve due to either experimental limitation to cool sample down to low enough reduced temperatures, T/T_c , either to create reasonably high applied magnetic field, $B_{\text{app}}/B_{c2}(0)$, or, in most cases, the both.

Based on this, the analysis of $B_{c2}(T)$ data, as a rule, performs by the utilization of other approaches, different from WHH [29,30], which were developed for real world experiments, i.e. when $B_{c2}(T)$ dataset is limited by measurements performed at high reduced temperatures,

$\frac{1}{2} \lesssim \frac{T}{T_c}$. We stress that this is entire case for highly compressed LaH₁₀ for which $B_{c2}(T)$ data is

available to date only in narrow temperature range of $0.96 \leq \frac{T}{T_c} \leq 1.0$ [21]. Primary reason for this is that available in experiment applied magnetic field was limited by $B_{appl} \leq 9 T$ [21], which is typical for modern labs (for instance, conventional PPMS systems provide this). However, if even world top quasi-DC magnetic field facility will be in use [15,16,31] and maximum applied magnetic field of $B_{appl} = 62 - 65 T$ will be utilized, then based on estimated value for $B_{c2}(0) = 90-140 T$ (given by Drozdov *et al* [21]) for LaH₁₀, it is unlikely that $B_{c2}(T)$ measurements will be possible to perform at reduced temperature lower than $0.7 \leq \frac{T}{T_c}$, i.e., $170 K \leq T$.

The reality is that robust use of WHH model [29,30] for highly compressed LaH₁₀ (and, probably, for others homological compounds of La_nH_m series [32,33]) will be unlikely in near decades. Thus, different models need to be used to analyse experimental $B_{c2}(T)$ data for near-room-temperature superconductors. One of the approach, which was actually proposed by Werthamer, Helfand, and Hohenberg [29,30], is extrapolative expression:

$$B_{c2}(0) = \frac{\phi_0}{2 \cdot \pi \cdot \xi^2(0)} = -0.693 \cdot T_c \cdot \left(\frac{dB_{c2}(T)}{dT} \right)_{T \sim T_c} \quad (3)$$

In this paper, we will designate Eq. 3 as WHH model.

Another model, which is also based on Werthamer, Helfand, and Hohenberg primary idea [29,30], but one accurately generates full $B_{c2}(T)$ extrapolative curve from experimental data measured at high reduced temperatures, T/T_c , was developed by Baumgartner *et al* [34]:

$$\begin{aligned} B_{c2}(T) &= B_{c2}(0) \cdot \left(\frac{\left(1 - \frac{T}{T_c}\right) - 0.153 \cdot \left(1 - \frac{T}{T_c}\right)^2 - 0.152 \cdot \left(1 - \frac{T}{T_c}\right)^4}{0.693} \right) = \\ &= \frac{\phi_0}{2 \cdot \pi \cdot \xi^2(0)} \cdot \left(\frac{\left(1 - \frac{T}{T_c}\right) - 0.153 \cdot \left(1 - \frac{T}{T_c}\right)^2 - 0.152 \cdot \left(1 - \frac{T}{T_c}\right)^4}{0.693} \right) \end{aligned} \quad (4)$$

We will designate this model as B-WHH model.

In addition, we will use classical two-fluid Gorter-Casimir model (GC model) [35,36]:

$$B_{c2}(T) = B_{c2}(0) \cdot \left(1 - \left(\frac{T}{T_c}\right)^2\right) = \frac{\phi_0}{2 \cdot \pi \cdot \xi^2(0)} \cdot \left(1 - \left(\frac{T}{T_c}\right)^2\right) \quad (5)$$

which is in a wide use too [1,15,21,37,38]. We note, that Drozdov *et al* [1], Mozaffari *et al* [15,16] and Drozdov *et al* [21] designate Eq. 5 as the Ginzburg-Landau theory equation [28].

This is incorrect, because the latter is [28,35]:

$$B_{c2}(T) = B_{c2}(0) \cdot \left(1 - \left(\frac{T}{T_c}\right)\right) = \frac{\phi_0}{2 \cdot \pi \cdot \xi^2(0)} \cdot \left(1 - \left(\frac{T}{T_c}\right)\right) \quad (6)$$

There is also $B_{c2}(T)$ model proposed by Gor'kov [39] which was written in analytical form by Jones *et al.* [40]:

$$B_{c2}(T) = B_{c2}(0) \cdot \left(\frac{1.77 - 0.43 \cdot \left(\frac{T}{T_c}\right)^2 + 0.07 \cdot \left(\frac{T}{T_c}\right)^4}{1.77}\right) \cdot \left[1 - \left(\frac{T}{T_c}\right)^2\right] = \frac{\phi_0}{2 \cdot \pi \cdot \xi^2(0)} \cdot \left(\frac{1.77 - 0.43 \cdot \left(\frac{T}{T_c}\right)^2 + 0.07 \cdot \left(\frac{T}{T_c}\right)^4}{1.77}\right) \cdot \left[1 - \left(\frac{T}{T_c}\right)^2\right] \quad (7)$$

III. Th₄H₁₅-Th₄D₁₅ superconductors in Uemura plot

We start our consideration with the first discovered superhydride superconductors, i.e., Th₄H₁₅ and Th₄D₁₅ [22]. We should note, that already in the first paper of 1970, Satterthwaite and Toepke [22] reported the absence of the isotope effect in ThH-ThD system:

$$T_c \cdot M^\alpha = const. \quad (8)$$

where M is isotope mass, and $\alpha \approx 1/2$ for weak-coupling limit of BCS theory [7], which is one of indispensable fundamental feature of electron-phonon mediated superconductivity [7]. Later, Stritzker and Buckel [41] experimentally found that the isotope effect in the palladium-hydrogen-deuterium (PdH-PdD) system has opposite sign (so called, reverse isotope effect). Yussouff *et al.* [42] extended this discovery on palladium-hydrogen-deuterium-tritium system (PdH-PdD-PdT). This reverse isotope effect in PdH-PdD-PdT system is still under wide discussion [43,44]. In regard of ThH-ThD system, detailed studied by Caton and

Satterthwaite [45] showed that superconductors in thorium-hydrogen-deuterium (ThH-ThD) system have also reverse isotope effect.

From the author knowledge, available to date experimental data for the upper critical field, $B_{c2}(T)$, are limited by values reported by Satterthwaite and Toepke [22]. The authors reported for both, Th_4H_{15} and Th_4D_{15} , compounds:

$$B_{c2}(T \sim 0) = 2.5 - 3.0 \text{ T}. \quad (9)$$

From these values, the ground state coherence length, $\xi(0)$, for Th_4H_{15} and Th_4D_{15} phases, can be derived as following:

$$\xi(0) = 11.0 \pm 0.5 \text{ nm} \quad (10)$$

Miller *et al.* [46] for both phases reported the BCS ratio within a range:

$$\alpha = \frac{2 \cdot \Delta(0)}{k_B \cdot T_c} = 3.42 - 3.47. \quad (11)$$

By utilizing superconducting transition temperature for Th_4H_{15} and Th_4D_{15} phases [22]:

$$T_c = 8.20 \pm 0.15 \text{ K} \quad (12)$$

one can deduce ground state superconducting energy gap:

$$\Delta(0) = 1.22 \pm 0.03 \text{ meV} \quad (13)$$

and by using well-known BCS expression [7]:

$$\xi(0) = \frac{\hbar \cdot v_F}{\pi \cdot \Delta(0)} \quad (14)$$

where $\hbar = h/2\pi$ is reduced Planck constant, one can calculate the Fermi velocity, v_F , in

Th_4H_{15} and Th_4D_{15} phases:

$$v_F = \pi \cdot \frac{\xi(0) \cdot \Delta(0)}{\hbar} = (6.4 \pm 0.2) \cdot 10^4 \text{ m/s} \quad (15)$$

To place Th_4H_{15} and Th_4D_{15} phases in the Uemura plot [18], we need to make assumption about the effective charge carrier mass, m_{eff}^* , to calculate the Fermi temperature, T_F :

$$T_F = \frac{\varepsilon_F}{k_B} = \frac{m_{eff}^* \cdot v_F^2}{2 \cdot k_B} \quad (16)$$

Due to there is no any available experimental values to date for Th_4H_{15} and Th_4D_{15} phases we used the simplest assumption:

$$m_{eff}^* = 1.0 \cdot m_e \quad (17)$$

and one can calculate the Fermi temperature, T_F :

$$T_F = \frac{\varepsilon_F}{k_B} = \frac{m_{eff}^* \cdot v_F^2}{2 \cdot k_B} = 137 \pm 9 \text{ K} \quad (18)$$

and the ratio:

$$\frac{T_c}{T_F} = 0.060 \pm 0.005 \quad (19)$$

which places both Th_4H_{15} and Th_4D_{15} phases in the upper boarder of the unconventional superconductor (Fig. 1).

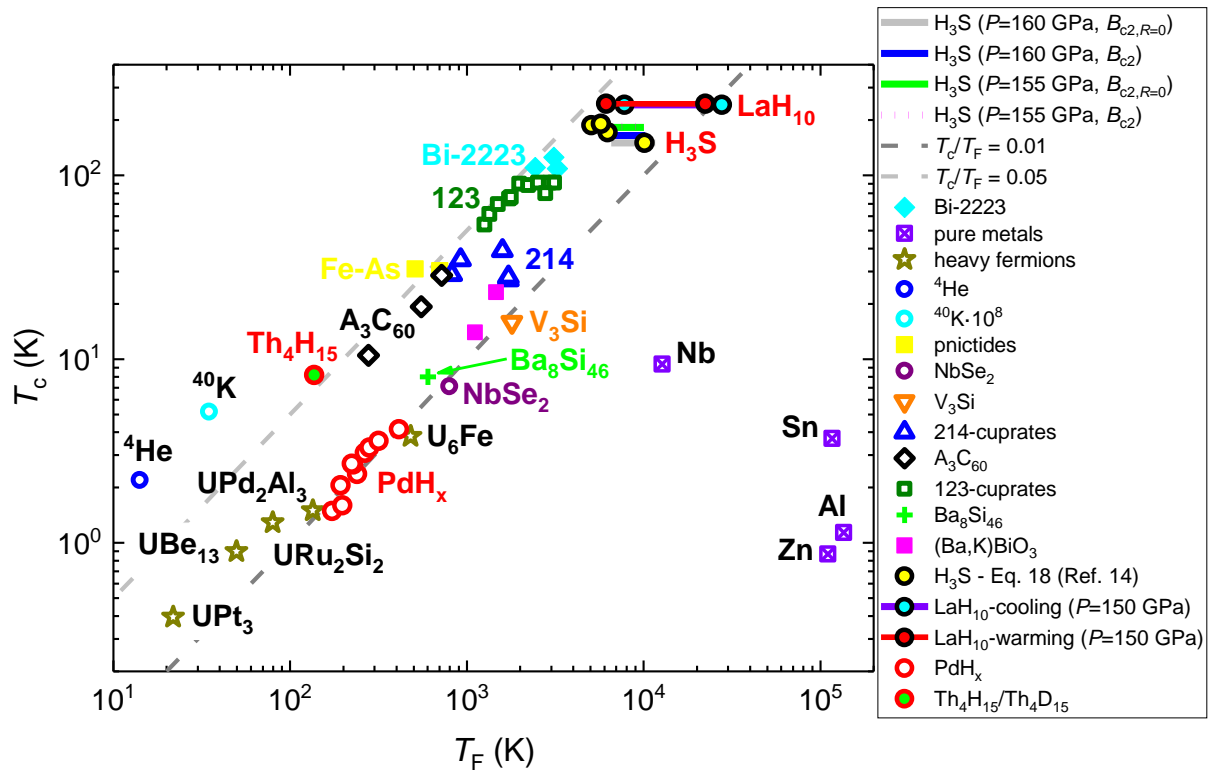


Figure 1. A plot of T_c versus T_F obtained for most representative superconducting families including PdH_x , H_3S and LaH_{10} . Data was taken from Uemura [18], Ye *et al.* [47], Qian *et al.* [48], Hashimoto *et al.* [49] and Ref. 14.

IV. PdH_x superconductors in Uemura plot

Surprisingly enough, to author's knowledge, as thorium-hydrogen-deuterium superconductors discovered by Satterthwaite and Toepke [22] in 1970, as palladium-hydrogen-deuterium superconductors discovered by Skoskiewicz [23] in 1973 have never been located in the Uemura plot [18]. To do this, we utilize results of systematic studies of the upper critical field for palladium-hydrogen superconductors reported by Balbaa and Manchester [50]. We show their results (i.e., T_c and $B_{c2}(0)$) in Table I together with calculated by using Eq. 1 values for $\xi(0)$.

Skoskiewicz [23] reported that PdH_x superconductors have the ratio:

$$\alpha = \frac{2 \cdot \Delta(0)}{k_B \cdot T_c} = 3.7 \quad (20)$$

where $\Delta(0)$ is ground state superconducting energy gap, k_B is the Boltzmann constant, which is very close to BCS weak-coupling limit of 3.53 [7]. Sansores *et al.* [51] performed the analysis of experimental electronic specific heat jump at T_c , $\Delta C/C$, and confirmed the weak-coupling pairing strength in PdH_x and PdD_x by reporting:

$$\frac{\Delta C}{C} = 1.44 - 1.59 \quad (21)$$

which is very close to BCS weak-coupling limit of 1.43 [7]. Thus, we use α value reported by Skoskiewicz (Eq. 8) [23] in our calculations below.

Bambakidis *et al.* [52] reported that PdD_x compounds have charge carrier effective mass of:

$$m_{eff}^* = 0.49 \cdot m_e \quad (22)$$

where m_e is electron mass, which we use in calculations below for PdH_x superconductors.

By using Eqs. 9-19 we calculate value which presented in Table I and Fig. 1.

Table I. Deduced parameters for PdH_x superconductors based on data reported by Balbaa and Manchester [50]. We assumed that $\frac{2\Delta(0)}{k_B T_c} = 3.7$ [23] and electron effective mass is $m_{eff}^* = 0.49 \cdot m_e$ [52]. Maximal and minimal T_c/T_F values are in red bold.

$x = \text{H/Pd}$	T_c (K)	$B_{c2}(0)$ (mT)	Deduced $\xi(0)$ (nm)	v_F (10^5 m/s)	$\Delta(0)$ meV	ϵ_F meV	$\Delta(0)/\epsilon_F$	T_F	T_c/T_F
0.821	1.488	39.5	91.3	1.03	0.237	14.9	0.016	173	0.009
0.826	1.600	40.0	90.8	1.11	0.255	15.0	0.015	198	0.008
0.843	2.061	68.0	69.6	1.09	0.329	16.6	0.020	193	0.011
0.852	2.365	72.0	67.6	1.22	0.377	20.6	0.018	239	0.010
0.862	2.672	96.5	58.4	1.19	0.426	19.6	0.022	228	0.012
0.863	2.695	100.0	57.4	1.18	0.430	19.3	0.022	224	0.012
0.875	3.090	111.0	54.5	1.28	0.493	22.9	0.022	265	0.012
0.881	3.305	120.0	52.4	1.32	0.527	24.2	0.022	281	0.012
0.887	3.590	125.0	51.3	1.40	0.572	27.4	0.021	317	0.011
0.905	4.158	129.0	50.5	1.60	0.663	35.6	0.019	413	0.010

It can be seen (Fig. 1) that PdH_x falls just next to heavy fermion superconductors and thus these hydrogen-rich superconductors should be classified as unconventional superconductors.

V. Deduced $B_{c2}(0)$ and $\xi(0)$ for compressed LaH₁₀

In Fig. 2,a we show raw $B_{c2}(T)$ data for compressed LaH₁₀ measured at the “cooling” stage (see for details Ref. 21). $B_{c2}(T)$ dataset was deduced from $R(T)$ curves showed in Fig. 2(a) of Drozdov *et al* [21] by using 50% of the normal state resistance criterion (raw data are given in Supplementary Table I). We note that Drozdov *et al* [21] also used this criterion to deduce $B_{c2}(T)$ and they also fitted data to Eq. 5 in their Fig. 2(b). In our Fig. 2,a we show fits to Eqs. 3-5,7 with deduced values collected in Table II.

For so-called “warming” stage, Drozdov *et al* [21] registered different $R(T)$ curves (Fig. 2(a) [21]) which we process in the same way and fit to Eqs. 3-5,7 (Fig. 2,b) (raw data are given in Supplementary Table II). Deduced $B_{c2}(0)$ and $\xi(0)$ values are collected in Table II.

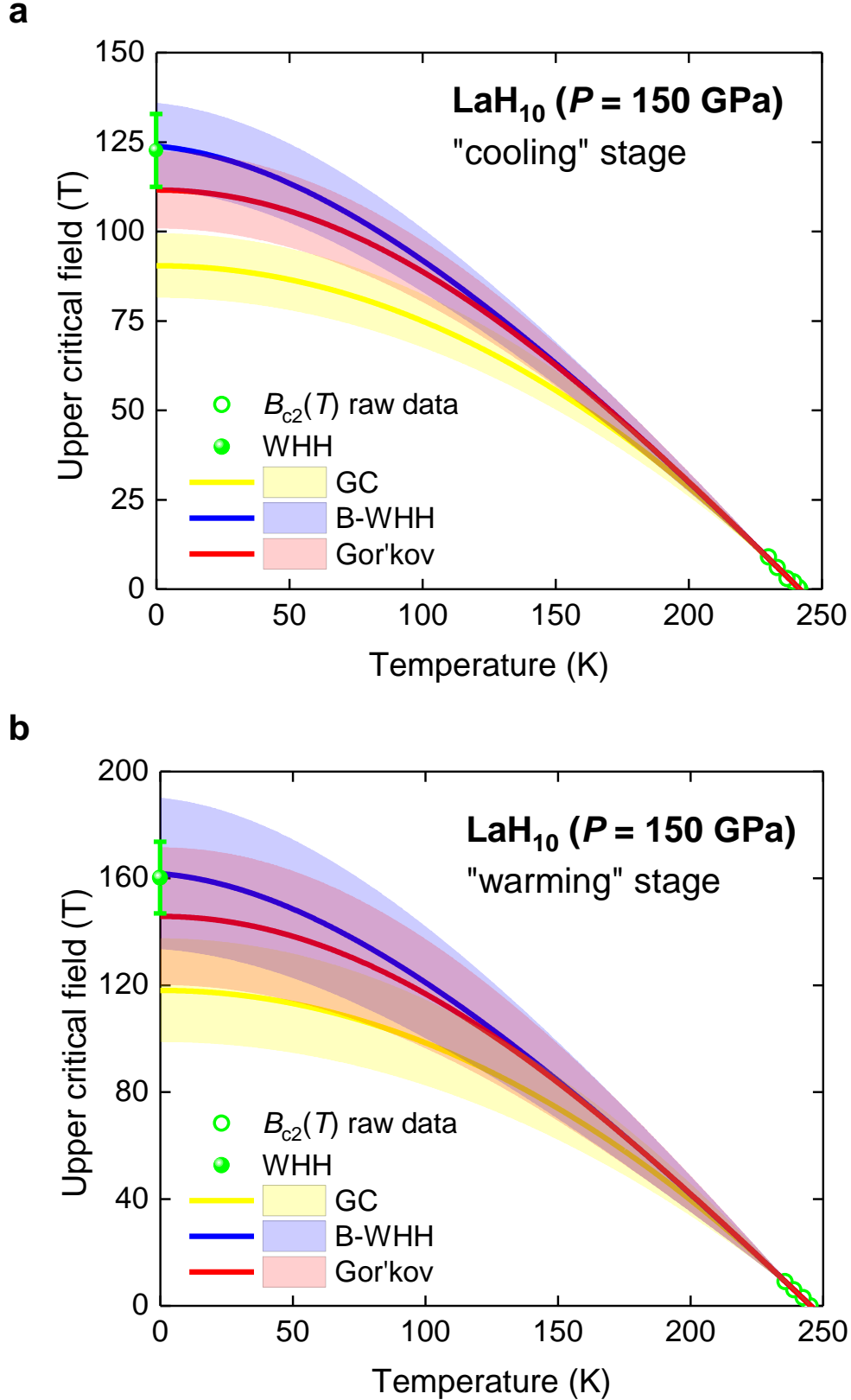


Figure 2. Superconducting upper critical field, $B_{c2}(T)$, data (magenta circles) and fits to four different model (Eqs. 3-5,7) for LaH₁₀ compressed at pressure $P = 150$ GPa (raw data are from Ref. 21) at (a) "cooling" and (b) "warming" stages. 95% confidence bars are shown.

IV. Compressed LaH₁₀ in Uemura plot

Kruglov *et al.* [33] performed first principles calculations and came to conclusion that compressed LaH₁₀ is strong coupled superconductor with the ratio:

$$\alpha = \frac{2 \cdot \Delta(0)}{k_B \cdot T_c} = 5.00 - 5.55 \quad (23)$$

where $\Delta(0)$ is ground state superconducting energy gap, k_B is the Boltzmann constant.

Despite a fact that the upper boundary for α is the highest ever reported for electron-phonon mediated superconductors [9] we use this value as maximal α amplitude in our calculations below (Table II and Fig. 1).

We note that first principles calculations performed for H₃S also showed high values for the ratio (references can be found elsewhere [4,9]):

$$\alpha = \frac{2 \cdot \Delta(0)}{k_B \cdot T_c} = 4.5 - 4.7 \quad (24)$$

Table II. Deduced parameters for LaH₁₀ superconductor subjected to external pressure of $P = 150$ GPa. We assumed that electron effective mass is $m_{eff}^* = 3.0 \cdot m_e$ [58]. Maximal and minimal T_c/T_F values are in red bold.

Stage	Model	Deduced T_c (K)	Deduced $\xi(0)$ (nm)	Assumed $\frac{2 \cdot \Delta(0)}{k_B \cdot T_c}$	v_F (10^5 m/s)	$\Delta(0)$ (meV)	ϵ_F (eV)	$\Delta(0)/\epsilon_F$	T_F (10^3 K)	T_c/T_F
cooling	B-WHH	241.7 ± 0.2	1.63 ± 0.03	3.53	2.9 ± 0.1	36.8 ± 0.1	0.70 ± 0.03	0.053 ± 0.002	8.1 ± 0.3	0.030 ± 0.001
				5.55	4.5 ± 0.1	57.8 ± 0.1	1.72 ± 0.06	0.034 ± 0.001	20.0 ± 0.8	0.012 ± 0.001
	GC	241.6 ± 0.2	1.91 ± 0.04	3.53	3.4 ± 0.1	36.7 ± 0.1	0.96 ± 0.04	0.038 ± 0.002	11.1 ± 0.5	0.022 ± 0.001
				5.55	5.3 ± 0.1	57.8 ± 0.1	2.40 ± 0.10	0.024 ± 0.002	27.5 ± 0.8	0.009 ± 0.001
	G	241.7 ± 0.2	1.72 ± 0.04	3.53	3.0 ± 0.1	36.8 ± 0.1	0.78 ± 0.04	0.047 ± 0.003	9.0 ± 0.4	0.027 ± 0.001
				5.55	4.7 ± 0.1	57.8 ± 0.1	1.92 ± 0.09	0.030 ± 0.002	22.3 ± 1.1	0.011 ± 0.001
warming	B-WHH	245.3 ± 0.2	1.43 ± 0.03	3.53	2.6 ± 0.1	37.3 ± 0.1	0.55 ± 0.02	0.068 ± 0.003	6.4 ± 0.3	0.038 ± 0.002
				5.55	4.0 ± 0.1	58.7 ± 0.1	1.37 ± 0.06	0.043 ± 0.002	15.9 ± 0.7	0.016 ± 0.001
	GC	245.3 ± 0.2	1.67 ± 0.03	3.53	3.0 ± 0.1	37.3 ± 0.1	0.75 ± 0.03	0.050 ± 0.003	8.8 ± 0.4	0.028 ± 0.001
				5.55	4.7 ± 0.1	58.7 ± 0.1	1.86 ± 0.09	0.032 ± 0.002	21.6 ± 0.9	0.011 ± 0.001
	G	245.3 ± 0.3	1.50 ± 0.03	3.53	2.7 ± 0.1	37.3 ± 0.1	0.61 ± 0.03	0.061 ± 0.004	7.1 ± 0.4	0.035 ± 0.002
				5.55	4.2 ± 0.1	58.7 ± 0.1	1.50 ± 0.06	0.039 ± 0.003	17.5 ± 0.7	0.014 ± 0.001

From other hand, Hirsch and Marsiglio [53], Souza and Marsiglio [54], Harshman and Fiory [55], Kaplan and Imry [56] proposed different models for the superconductivity in H₃S either within classical BCS approach [56], either based on new concepts, and, for instance, Kaplan and Imry [56] showed that their model gives α within weak-coupling BCS limit:

$$\alpha = \frac{2 \cdot \Delta(0)}{k_B \cdot T_c} = 3.53 \quad (25)$$

This α value is in a good agreement with ones we deduced from experimental $B_{c2}(T)$ [14] and the self-field critical current density, $J_c(\text{sf}, T)$, data [57]. Assuming that both hydrogen-rich counterparts (H₃S and LaH₁₀) have the same origin for near-room-temperature superconductivity, we calculated parameters for the latter (Table II and Fig. 1) by using weak-coupling limit of BCS (Eq. 25) as the lowest value for α .

Kostrzewa *et al.* [58] reported that at $P = 150$ GPa compressed LaH₁₀ has charge carrier effective mass of:

$$m_{eff}^* = (2.9 - 3.2) \cdot m_e \approx 3.0 \cdot m_e \quad (26)$$

where m_e is electron mass. This value is very close to $m_{eff}^* = 2.76 \cdot m_e$ calculated for compressed H₃S by Durajski [11]. For the simplicity, in our calculations below, for compressed LaH₁₀ we use rounded value of $m_{eff}^* = 3.0 \cdot m_e$.

We perform the same calculation routine to one as we did for PdH_x and calculated values are given in Table II and displayed in Fig. 1. Deduced T_c/T_F values are in the range of $0.9 \cdot 10^{-2} < T_c/T_F < 4.0 \cdot 10^{-2}$. It can be seen (Fig. 1) that LaH₁₀ falls just above another hydrogen-rich counterpart, H₃S, and both near-room-temperature superconductors are placed in unconventional superconductors band together with heavy fermions, PdH_x, fullerenes, pnictides and cuprates.

More evidently our primary conclusion that H₃S and LaH₁₀ are unconventional superconductors can be understood if one substitutes Eqs. 9-19 in the equation Eq. 1 and obtains:

$$B_{c2} \left(\frac{T}{T_c} = 0 \right) = \frac{\pi \cdot \phi_0 \cdot k_B}{16 \cdot \hbar^2} \cdot m_{eff}^* \cdot \alpha^2 \cdot \left(\frac{T_c}{T_F} \right) \cdot T_c, \quad (27)$$

If LaH₁₀ will be a conventional superconductor with $T_c/T_F = 8.4 \cdot 10^{-6}$ (this is the ratio of electron-phonon mediated Al [18]), then in accordance with Eq. 27:

$$B_{c2} \left(\frac{T}{T_c} = 0 \right) = 70 \text{ mT} \quad (28)$$

If $T_c/T_F = 7.4 \cdot 10^{-4}$ (which is the ratio of electron-phonon mediated Nb [18]), then:

$$B_{c2} \left(\frac{T}{T_c} = 0 \right) = 6.2 \text{ T} \quad (29)$$

We note, that experimental $B_{c2}(T)$ value for LaH₁₀ [21] is:

$$B_{c2} \left(\frac{T}{T_c} = 0.96 \right) = 9.0 \text{ T} \quad (30)$$

Thus, Eqs. 27-30 show that despite a fact that currently $B_{c2}(T)$ dataset for LaH₁₀ is available only at temperatures near T_c (i.e., $0.96 \leq \frac{T}{T_c} \leq 1.0$), this dataset is already enough to make a conclusion that LaH₁₀ is unconventional superconductor.

Similar calculations for H₃S (based on experimental [15,16] and deduced [14] values) are:

$$B_{c2} \left(\frac{T}{T_c} = 0 \right) < 45 \text{ mT} \quad (\text{H}_3\text{S for } T_c/T_F = 8.4 \cdot 10^{-6}) \quad (31)$$

$$B_{c2} \left(\frac{T}{T_c} = 0 \right) < 3.9 \text{ T} \quad (\text{H}_3\text{S for } T_c/T_F = 7.4 \cdot 10^{-4}). \quad (32)$$

These values (if even we will make comparison of ones with very strictly defined $B_{c2}(T)$ (at $R = 0 \Omega$) and pressure of $P = 160 \text{ GPa}$ (which is shifted from optimal pressure of $P = 155 \text{ GPa}$)) are at least in one order of magnitude lower than experimental data:

$$B_{c2} \left(\frac{T}{T_c} \approx \frac{1}{3} \right) = 65 \text{ T} \quad (\text{H}_3\text{S at } P = 160 \text{ GPa}). \quad (33)$$

Eqs. 27-33 show that both near-room-temperature superconductors, H₃S and LaH₁₀, cannot be classified as conventional superconductors, despite a fact that astonishing Ashcroft's prediction [59,60] about near-room-temperature superconductivity in hydrogen-rich compounds was based on BCS theory.

In overall, all extrapolated $B_{c2}(0)$ values for LaH₁₀ (Fig. 2) are well below the Pauli depairing field of:

$$B_p(0) = \frac{2 \cdot \Delta(0)}{g \cdot \mu_B} = \alpha \cdot \frac{k_B \cdot T_c}{g \cdot \mu_B} = 630 - 1,000 T \gg B_{c2}(0) \quad (34)$$

where $g = 2$ and $\mu_B = \frac{e \cdot \hbar}{2 \cdot m_e}$ is the Bohr magneton. According to Gor'kov's note [61], Eq. 34 means that the mean-free path, l , of the electrons is large compared with the coherence length, $\xi(0)$:

$$l \gg \xi(T) > \xi(0) \sim 1.4 - 1.9 \text{ nm} \quad (35)$$

However, the lower limit for the mean-free path, l , is only in a few times exceeded the lattice constants for any structural unit cell of LaH₁₀ either proposed by first principles calculations [33], either deduced by the fits of experimental data to $Fm-3m$ symmetry ($a = 0.51019(5)$ nm [21]) or $P4/nmm$ symmetry ($a = 0.37258(6)$ nm, $c = 0.50953(12)$ nm [21]). This means that charge carrier scattering is large in LaH₁₀.

V. Thermodynamic fluctuations in compressed LaH₁₀

In our previous papers [57,62] we answered a question about possible limitation of T_c in compressed H₃S by the thermodynamic fluctuations of the order parameter. There are phase [63] and amplitude [64] fluctuations of the order parameter in superconductors. These fluctuations for the case of three dimensional (3D) superconductors (like, Th₄H₁₅, PdH_x, H₃S and LaH₁₀) have characteristic temperatures:

$$T_{fluc,phase} = \frac{0.55 \cdot \phi_0^2}{\pi^{3/2} \cdot \mu_0 \cdot k_B} \cdot \frac{1}{\kappa^2 \cdot \xi(0)} \quad (36)$$

$$T_{fluc,amp} = \frac{\phi_0^2}{12 \cdot \pi \cdot \mu_0 \cdot k_B} \cdot \frac{1}{\kappa^2 \cdot \xi(0)} \quad (37)$$

where $\kappa = \lambda(0)/\xi(0)$ is the Ginzburg-Landau parameter, and $\lambda(0)$ is the ground state London penetration depth.

Due to for Th_4H_{15} and Th_4D_{15} phases the Ginzburg-Landau parameter is unknown we do not consider this interesting case herein.

For PdH_x system, κ was found to be $\kappa = 1.2\text{-}2.0$ [50], and calculated values for $T_{fluc,phase}$ and $T_{fluc,amp}$ show that thermodynamic fluctuations for superconductors in palladium-hydrogen system are negligible low (Table III).

In our recent paper [14], we deduced $\xi(0)$ in H_3S more accurately in comparison with values we used to calculate $T_{fluc,phase}$ and $T_{fluc,amp}$ in our previous papers [57,62]. By taking in account that H_3S exhibits $\kappa = 88\text{-}105$ [57,62,65], we revisited $T_{fluc,phase}$ and $T_{fluc,amp}$ at two applied pressures of $P = 155$ GPa and 160 GPa (Table III). At each pressure, we used maximal and minimal deduced $\xi(0)$ values to show the range of variation for $T_{fluc,phase}$ and $T_{fluc,amp}$.

To calculate $T_{fluc,phase}$ and $T_{fluc,amp}$ (Eqs. 36,37) for compressed LaH_{10} there is a need to make an assumption about the value for Ginzburg-Landau parameter, κ . Our approach is based on an assumption that κ for LaH_{10} will be not much different from κ for H_3S and other unconventional superconductors (primarily, pnictides and cuprates) which have values within a range of $\kappa = 60\text{-}120$ [65-71]. Calculated $T_{fluc,phase}$ and $T_{fluc,amp}$ for LaH_{10} are given in Table III.

Examination of the values in Table III led us to an important finding that both near-room-temperature superconductors have very large fluctuations of the order parameter amplitude, which, in some scenarios, have characteristic temperatures, $T_{fluc,amp}$, of only about 15% above observed transition temperature, T_c . This is similar to cuprates and pnictides

which have large fluctuations of order parameter phase [57,62] (which causes the suppression of the observed T_c by about 30% from its mean-field value, $T_c^{mean-field}$ [57,62]).

Table III. Calculated fluctuation temperatures for H₃S (at $P = 155$ and 160 GPa) and LaH₁₀ ($P = 150$ GPa). Assumed electron effective masses are $m_{eff}^* = 2.76 \cdot m_e$ [11] for H₃S and $m_{eff}^* = 3.0 \cdot m_e$ for LaH₁₀ [50]. The largest ratios for $\frac{T_c}{T_{fluc,phase}}$ and $\frac{T_c}{T_{fluc,amp}}$ are marked in red bold. Deduced T_c and $\xi(0)$ values for H₃S are from Ref. 14.

Material	Stage	Pressure (GPa)	Deduced T_c (K)	Deduced $\xi(0)$ (nm)	Assumed κ	$T_{fluc,phase}$ (K)	$T_{fluc,amp}$ (K)	$T_c/T_{fluc,phase}$	$T_c/T_{fluc,amp}$		
PdH _x	N/A	N/A	4.16	50.5	2	$1.2 \cdot 10^5$	$3.2 \cdot 10^4$	$3.5 \cdot 10^{-5}$	$1.3 \cdot 10^{-4}$		
H ₃ S	N/A	155	182 ± 1	1.97 ± 0.02	88	1590 ± 20	428 ± 5	0.114 ± 0.001	0.43 ± 0.01		
					105	1120 ± 11	304 ± 5	0.163 ± 0.002	0.61 ± 0.01		
			189 ± 1	1.68 ± 0.01	88	1870 ± 10	502 ± 3	0.101 ± 0.001	0.38 ± 0.01		
					105	1313 ± 11	353 ± 5	0.144 ± 0.001	0.54 ± 0.01		
		160	150 ± 3	2.67 ± 0.05	88	1176 ± 23	316 ± 6	0.128 ± 0.003	0.48 ± 0.01		
					105	826 ± 16	222 ± 4	0.182 ± 0.004	0.68 ± 0.02		
			172 ± 2	2.06 ± 0.01	88	1524 ± 8	410 ± 2	0.113 ± 0.001	0.42 ± 0.01		
					105	1071 ± 5	288 ± 2	0.161 ± 0.002	0.60 ± 0.01		
		LaH ₁₀	cooling	150	241.7 ± 0.2	1.63 ± 0.03	60	4150 ± 70	1113 ± 30	0.058 ± 0.001	0.21 ± 0.01
							120	1036 ± 20	278 ± 6	0.233 ± 0.004	0.87 ± 0.02
warming	150		245.3 ± 0.2	1.43 ± 0.03	60	4720 ± 100	1270 ± 30	0.052 ± 0.001	0.19 ± 0.01		
					120	1180 ± 25	317 ± 7	0.208 ± 0.005	0.77 ± 0.02		

VI. Self-field critical currents in compressed LaH₁₀

We need to stress, that there is fundamental limit to obtain answers on many important questions in regards of H₃S and LaH₁₀ by performing the upper critical field studies, because experimentally available magnetic fields, B_{app} , even, if top world facilities will be in use [15,16,31], are too low for these materials. Thus, there is a need to find different experimental techniques to reveal the nature of superconductivity in these and, perhaps, many others near-room-temperature hydrogen-based superconductors. One possible way to perform

this is to study temperature dependent self-field critical currents, $I_c(\text{sf}, T)$ [37,65], from which several fundamental parameters of the superconductor, i.e., the ground state superconducting energy gap, $\Delta(0)$, the ground state London penetration depth, $\lambda(0)$, and relative jump in the specific heat at T_c , $\Delta C/C$, can be deduced. We already showed that this approach works for compressed H_3S [57] by performing analysis of the self-field magnetization critical current densities reported by Drozdov *et al.* [1].

We note that experimental technique to perform critical current measurements in ultrahigh-pressure diamond cells is under developing for about twenty years [72-75] and fundamental possibility to measure $I_c(\text{sf}, T)$ in LaH_{10} has been already demonstrated by Somayazulu *et al* [20] in their Fig. 4 and Supplementary Information. However, $I_c(\text{sf}, T)$ measurement techniques (and particularly inside of ultrahigh-pressure diamond cells) need to be further developed, because these measurements require great precaution due to the danger of sample “burning” during transport current pulse [76-78], and $I_c(\text{sf}, T)$ data collecting is still state-of-art [79,80]. For instance, LaH_{10} samples degradation, after $I_c(\text{sf}, T)$ measurements reported by Somayazulu *et al* [20], is more likely originated from the sample “burning” under transport current flow. In this regard, recently registered effect [81] of the linearization of surface magnetic field, $B_{\text{surf}}(I)$, vs transport current rise at the onset of power dissipation can be considered as a new option. We showed recently, that this effect [81,82] works when external magnetic field, B_{appl} , is applied to the sample [83,84].

There are also two powerful optical spectroscopy techniques, one is the Raman spectroscopy (which is under on-going developing to be used in ultrahigh-pressure diamond cells for last decades [85-88]), and another is the angle resolved photoemission spectroscopy (ARPES) which was recently advanced [89] to be applicable to study superconducting films under transport current flow.

VII. Conclusions

In this paper we analyse experimental $B_{c2}(T)$ data of near-room-temperature superconductor, LaH_{10} (recently reported by Drozdov *et al.* [21]), of palladium-hydrogen superconductors, PdH_x (reported by Balbaa and Manchester [50]) and of Th_4H_{15} - Th_4D_{15} (reported by Satterthwaite and Toepke [22]). We come to conclusion that all discovered to date hydrogen-rich superconductors for which fundamental superconducting parameters beyond T_c were measured (in this list we do not include NbTiH_x , PtH_x , SiH_4 and PH_3 for which only experimental T_c vs pressure are known), i.e., Th_4H_{15} - Th_4D_{15} , PdH_x , H_3S and LaH_{10} , are unconventional superconductors.

In addition, we find that both near-room-temperature superconductors, H_3S and LaH_{10} , are subjected by strong thermodynamic fluctuations of the order parameter amplitude. We note, that this is very similar to pnictides and cuprates in which superconducting state is affected by strong fluctuations of the order parameter phase.

Acknowledgement

Author thanks Prof. V. E. Antonov (Institute of Solid State Physics, Russian Academy of Sciences) and Prof. E. Gregoryanz (University of Edinburgh) for valuable discussions.

Author also thanks financial support provided by the state assignment of Minobrnauki of Russia (theme “Pressure” No. AAAA-A18-118020190104-3) and by Act 211 Government of the Russian Federation, contract No. 02.A03.21.0006.

References

- [1] Drozdov A P, Erements M I, Troyan I A, Ksenofontov V, Shylin S I 2015 Conventional superconductivity at 203 kelvin at high pressures in the sulfur hydride system *Nature* **525** 73-76
- [2] Bednorz J G and Mueller K A 1986 Possible high T_c superconductivity in the Ba-La-Cu-O system *Z. Phys. B* **64** 189-193

- [3] Eremets M I and Drozdov A P 2016 High-temperature conventional superconductivity *Phys.-Usp.* **59** 1154-1160
- [4] Gor'kov L P and Kresin V Z 2018 *Colloquium: High pressure and road to room temperature superconductivity* *Rev. Mod. Phys.* **90** 011001
- [5] Pickett W and Eremets M I 2019 The quest for room-temperature superconductivity in hydrides *Physics today* **72** 52-58
- [6] Flores-Livas J A, Boeri L, Sanna A, Profeta G, Arita R, Eremets M 2019 A perspective on conventional high-temperature superconductors at high pressure: Methods and materials *arXiv:1905.06693*
- [7] Bardeen J, Cooper L N, Schrieffer J R 1957 Theory of superconductivity *Phys. Rev.* **108**, 1175-1204
- [8] Mazin I I 2015 Extraordinarily conventional *Nature* **525** 40-41
- [9] Nicol E J and Carbotte J P 2015 Comparison of pressurized sulfur hydride with conventional superconductors *Phys. Rev. B* **91** 220507(R)
- [10] Errea I *et al* 2015 High-pressure hydrogen sulfide from first principles: A strongly anharmonic phonon-mediated superconductor *Phys. Rev. Lett.* **114** 157004
- [11] Durajski A P 2016 Quantitative analysis of nonadiabatic effects in dense H₃S and PH₃ superconductors *Scientific Reports* **6** 38570
- [12] Jarlborg T and Bianconi A 2016 Breakdown of the Migdal approximation at Lifshitz transitions with giant zero-point motion in the H₃S superconductor *Scientific Reports* **6** 24816
- [13] Durajski A P and Szczeniński R 2018 Structural, electronic, vibrational, and superconducting properties of hydrogenated chlorine *J. Chem. Phys.* **149** 074101
- [14] Talantsev E F 2019 Classifying superconductivity in compressed H₃S *Modern Physics Letters B* **33** 1950195
- [15] Mozaffari S, *et al* 2019 Superconducting hydride under extreme field and pressure *Los Alamos National Laboratory Report LA-UR-18-30460*, doi: 10.2172/1481108.
- [16] Mozaffari S, *et al* 2019 Superconducting phase-diagram of H₃S under high magnetic fields *Nature Communications* **10** 2522
- [17] Uemura Y J, *et al* 1989 Universal correlations between T_c and $\frac{n_s}{m^*}$ (carrier density over effective mass) in high- T_c cuprate *Phys. Rev. Lett.* **62** 2317-2320
- [18] Uemura Y J 2004 Condensation, excitation, pairing, and superfluid density in high- T_c superconductors: the magnetic resonance mode as a roton analogue and a possible spin-mediated pairing *J. Phys.: Condens. Matter* **16** S4515-S4540
- [19] Hirsch J E, Maple M B, Marsiglio F 2015 Superconducting materials classes: Introduction and overview *Physica C* **514** 1-8
- [20] Somayazulu M, Ahart M, Mishra A K, Geballe Z M, Baldini M, Meng Y, Struzhkin V V and R. J. Hemley R J 2019 Evidence for superconductivity above 260 K in lanthanum superhydride at megabar pressures *Phys. Rev. Lett.* **122** 027001
- [21] Drozdov A P, *et al* 2019 Superconductivity at 250 K in lanthanum hydride under high pressures *Nature* **569** 528-531
- [22] Satterthwaite C B and Toepke I L 1970 Superconductivity of hydrides and deuterides of thorium *Phys. Rev. Lett.* **25** 741-743
- [23] Skoskiewicz T 1973 Superconductivity in the palladium-hydrogen system *Phys. Stat. Sol. (b)* **59** 329
- [24] Eremets M I, Trojan I A, Medvedev S A, Tse J S, Yao Y 2008 Superconductivity in hydrogen dominant materials: Silane *Science* **319** 1506-1509
- [25] Drozdov A P, Eremets M I, Troyan I A 2015 Superconductivity above 100 K in PH₃ at high pressures *arXiv:1508.06224*
- [26] Matsuoka T, *et al.* 2019 Superconductivity of platinum hydride *Phys Rev B* **99** 144511

- [27] Antonov V E, Belash I T, Zakharov M S, Orlov V A, Rashupkin V I 1986 *Int. J. Hydrogen Energy* **11** 475.
- [28] Ginzburg V L and Landau L D 1950 On the theory of superconductivity *Zh. Eksp. Teor. Fiz.* **20** 1064-1082
- [29] Helfand E and Werthamer N R 1966 Temperature and purity dependence of the superconducting critical field, H_{c2} . II. *Phys. Rev.* **147** 288-294
- [30] Werthamer N R, Helfand E and Hohenberg P C 1966 Temperature and purity dependence of the superconducting critical field, H_{c2} . III. Electron spin and spin-orbit effects *Phys. Rev.* **147** 295-302
- [31] Hänisch J, *et al.* 2015 High field superconducting properties of $\text{Ba}(\text{Fe}_{1-x}\text{Co}_x)_2\text{As}_2$ thin films *Sci. Rep.* **5** 17363
- [32] Liu H, Naumov I I, Hoffmann R, Ashcroft N W and Hemley R J 2017 Potential high- T_c superconducting lanthanum and yttrium hydrides at high pressure *Proc. Natl. Acad. Sci.* **114** 6990-6995
- [33] Kruglov I A, *et al.* 2019 Superconductivity of LaH_{10} and LaH_{16} : new twists of the story arXiv:1810.01113
- [34] Baumgartner T, Eisterer M, Weber H W, Fluekiger R, Scheuerlein C, Bottura L 2014 Effects of neutron irradiation on pinning force scaling in state-of-the-art Nb_3Sn wires *Supercond. Sci. Technol.* **27** 015005
- [35] Gorter C J and H. Casimir H 1934 On supraconductivity I *Physica* **1** 306-320
- [36] Poole P P, Farach H A, Creswick R J, Prozorov R 2007 Superconductivity (2-nd Edition, London, UK).
- [37] Talantsev E F, Crump W P, Island J O, Xing Y, Sun Y, Wang J, J. L. Tallon J L 2017 *2D Materials* **4** 025072
- [38] Pal B, *et al.* 2019 Experimental evidence of a very thin superconducting layer in epitaxial indium nitride *Supercond. Sci. Technol.* **32** 015009
- [39] Gor'kov L P 1960 The critical supercooling field in superconductivity theory *Soviet Physics JETP* **10** 593-599
- [40] Jones C K, Hulm J K, Chandrasekhar B S 1964 Upper critical field of solid solution alloys of the transition elements *Rev. Mod. Phys.* **36** 74-76
- [41] Stritzker B and Buckel W 1972 Superconductivity in the palladium-hydrogen and the palladium-deuterium systems *Zeitschrift für Physik A Hadrons and nuclei* **257** 1-8
- [42] Yussouff M, Rao B K and Jena P 1995 Reverse isotope effect on the superconductivity of PdH, PdD, and PdT *Solid State Communications* **94** 549-553
- [43] Villa-Cortés S and Baquero R 2018 On the calculation of the inverse isotope effect in PdH(D): A Migdal-Eliashberg theory approach *Journal of Physics and Chemistry of Solids* **119** 80-84
- [44] Ostanin S, Borisov V, Fedorov D V, Salamatov E I, Ernst A and Mertig I 2019 Role of tetrahedrally coordinated dopants in palladium hydrides on their superconductivity and inverse isotope effect *Journal of Physics: Condensed Matter* **31** 075703
- [45] Caton R and Satterthwaite C B 1977 Preparation and characterization of massive Th_4H_{15} and Th_4D_{15} *Journal of the Less Common Metals* **52** 307
- [46] Miller J F, Caton R H, Satterthwaite C B 1976 Low-temperature heat capacity of normal and superconducting thorium hydride and thorium deuteride. *Phys. Rev. B* **14** 2795
- [47] Ye J T, *et al.* 2012 Superconducting dome in a gate-tuned band insulator *Science* **338** 1193
- [48] Qian T, *et al.* 2011 Absence of a holelike Fermi surface for the iron-based $\text{K}_{0.8}\text{Fe}_{1.7}\text{Se}_2$ superconductor revealed by angle-resolved photoemission spectroscopy *Phys. Rev. Lett.* **106** 187001

- [49] Hashimoto K, Cho K, Shibauchi T, Kasahara S, Mizukami Y, Katsumata R, Tsuruhara Y, Terashima T, Ikeda H, Tanatar M A, Kitano H, Salovich N, Giannetta R W, Walmsley P, Carrington A, Prozorov R, Matsuda Y 2012 A sharp peak of the zero-temperature penetration depth at optimal composition in $\text{BaFe}_2(\text{As}_{1-x}\text{P}_x)_2$ *Science* **336** 1554-1557
- [50] Balbaa I S and Manchester F D 1983 Superconductivity of PdH_x in relation to its phase diagram: I. Magnetic measurements *J. Phys. F: Met. Phys.* **13** 395-404
- [51] Sansores L E, Taguena-Martinez J and Sanchez A M 1981 The specific heat and critical magnetic field of superconducting PdH(D) *Journal of Low Temperature Physics* **43** 205-215
- [52] Bambakidis G, Smith R J, and Otterson D A 1968 Electrical resistivity as a function of deuterium concentration in palladium *NASA Report Number TN D-4970*
- [53] Hirsch J E and Marsiglio F 2015 Hole superconductivity in H_2S and other sulfides under high pressure *Physica C* **511** 45-49
- [54] Souza T X R and Marsiglio F 2016 Systematic study of the superconducting critical temperature in two- and three-dimensional tight-binding models: A possible scenario for superconducting H_3S *Phys. Rev. B* **94** 184509
- [55] Harshman D R and Fiory A T 2017 Compressed H_3S : inter-sublattice Coulomb coupling in a high- T_c superconductor *J. Phys.: Condens. Matter* **29** 445702
- [56] Kaplan D and Imry Y 2018 High-temperature superconductivity using a model of hydrogen bonds *Proc. Nat. Acad. Sci.* **115** 5709-5713
- [57] Talantsev E F, Crump W P, Storey J G, Tallon J L 2017 London penetration depth and thermal fluctuations in the sulphur hydride 203 K superconductor *Annalen der Physics* **529** 1600390
- [58] Kostrzewa M, Szczesniak K M, Durajski A P, Szczesniak R 2019 From LaH_{10} to room-temperature superconductors arXiv:1905.12308
- [59] Ashcroft N W 1968 Metallic hydrogen: A high-temperature superconductor? *Phys. Rev. Lett.* **21** 1748-1749
- [60] Ashcroft N W 2004 Hydrogen dominant metallic alloys: High temperature superconductors? *Phys. Rev. Lett.* **92** 187002
- [61] Gor'kov L P 1963 An estimate of the limiting values of the critical fields for hard superconductors *Soviet Physics JETP* **17** 518
- [62] Tallon J L and Talantsev E F 2018 Compressed H_3S , superfluid density and the quest for room-temperature superconductivity *Journal of Superconductivity and Novel Magnetism* **31** 619-624
- [63] Emery V J and Kivelson S A 1995 Importance of phase fluctuations in superconductors with small superfluid density *Nature* **374** 434-437
- [64] Bulaevskii L N, Ginzburg V L, Sobyenin A A 1988 Macroscopic theory of superconductors with small coherence length *Physica C* **152** 378-388
- [65] Talantsev E F, Crump W P, Tallon J L 2017 Thermodynamic parameters of single- or multi-band superconductors derived from self-field critical currents *Annalen der Physics* **529** 1700197
- [66] Sakoda M, Iida K and Naito M 2018 Recent progress in thin-film growth of Fe-based superconductors: Superior superconductivity achieved by thin films *Supercond. Sci. Technol.* **31** 093001.
- [67] Iida K, Hänisch J, and Tarantini C 2018 Fe-based superconducting thin films on metallic substrates: Growth, characteristics, and relevant properties *Applied Physics Reviews* **5** 031304.
- [68] Eisterer M 2018 Radiation effects on iron-based superconductors *Supercond. Sci. Technol.* **31** 013001

- [69] Kauffmann-Weiss S *et al.* 2019 Microscopic origin of highly enhanced current carrying capabilities of thin NdFeAs(O,F) films *Nanoscale Advances* **1** 147
<https://doi.org/10.1039/C9NA00147F>
- [70] Hänisch J *et al.* 2019 Fe-based superconducting thin films – Preparation and tuning of superconducting properties *Supercond. Sci. Technol.* in press <https://doi.org/10.1088/1361-6668/ab1c00>
- [71] Talantsev E F 2019 Evaluation of practical level of critical current densities in pnictides and recently discovered superconductors *Supercond. Sci. Technol.* **32** 084007
- [72] Timofeev Y A, Struzhkin V V, Hemley R J, Mao H-K and Gregoryanz E A 2002 Improved techniques for measurement of superconductivity in diamond anvil cells by magnetic susceptibility *Rev. Sci. Instrum.* **73** 371
- [73] Eremets M I, Struzhkin V V, Mao H-K, Hemley R J 2003 Exploring superconductivity in low-Z materials at megabar pressures *Physica B: Condensed Matter* **329-333** 1312-1316
- [74] Gavriluk A G, Mironovich A A, and Struzhkin V V 2009 Miniature diamond anvil cell for broad range of high pressure measurements *Rev. Sci. Instrum.* **80** 043906
- [75] Guo J, Wu Q, and Sun L 2018 Advanced high-pressure transport measurement system integrated with low temperature and magnetic field *Chin. Phys. B* **27** 077402
- [76] Talantsev E F, Strickland N M, Hoefakker P, Xia J A, Long N J 2008 Critical current anisotropy for second generation HTS wires *Current Applied Physics* **8** 388-390
- [77] Strickland N M, Hoffmann C, Wimbush S C, Pooke D M, Huang T, Lazic Z, Chamritski V, Talantsev E F, Long N J and Tallon J L 2014 Cryogen-free 1kA-class I_c measurement system featuring an 8 T HTS magnet *J. Phys. Conf. Ser.* **507** 022037
- [78] Lao M, Hänisch J, Kauffmann-Weiss S, Gehring R, Fillinger H, Drechsler A, Holzapfel B 2019 High current variable temperature electrical characterization system for superconducting wires and tapes with continuous sample rotation in a split coil magnet *Review of Scientific Instruments* **90** 015106
- [79] Talantsev E F and Mataira R C 2018 Polar projections for big data analysis in applied superconductivity *AIP Advances* **8** 075213
- [80] Strickland N M, Hoffmann C, Wimbush S C 2014 *Review of Scientific Instruments* **85** 113907
- [81] Talantsev E F 2017 On the fundamental definition of critical current in superconductors *arXiv:1707.07395*
- [82] Talantsev E F, Strickland N M, Wimbush S C, Crump W P 2017 The onset of dissipation in high-temperature superconductors: Self-field experiments *AIP Advances* **7** 125230
- [83] Talantsev E F, Strickland N M, Wimbush S C, Brooks J, Pantoja A E, Badcock R A, Storey J G, Tallon J L 2018 The onset of dissipation in high-temperature superconductors: magnetic hysteresis and field dependence *Scientific Reports* **8** 14463
- [84] Talantsev E F and Brooks J 2019 The onset of dissipation in high-temperature superconductors: flux trap, hysteresis and in-field performance of multifilamentary $\text{Bi}_2\text{Sr}_2\text{Ca}_2\text{Cu}_3\text{O}_{10+x}$ wires *Mater. Res. Express* **6** 026002
- [85] Goncharov A F, Gregoryanz E, Mao H-K, Liu Z and Hemley R J 2000 Optical evidence for a nonmolecular phase of nitrogen above 150 GPa *Phys. Rev. Lett.* **85** 1262-1265
- [86] Chen X-A, *et al.* 2008 Pressure-induced metallization of silane *Proc. Natl. Acad. Sci. USA* **105** 20-23
- [87] Yuan Y, *et al.* 2019 Stoichiometric evolutions of PH_3 under high pressure: implication for high- T_c superconducting hydrides *National Science Review* **6** 524-531
- [88] Dalladay-Simpson P, *et al.* 2019 Band gap closure, incommensurability and molecular dissociation of dense chlorine *Nature Communications* **10** 1134

[89] Kaminski, A, Rosenkranz S, Norman M R, Randeria M, Li Z Z, Raffy H, and Campuzano J C 2016 Destroying coherence in high-temperature superconductors with current flow *Phys. Rev. X* **6** 031040

SUPPLEMENTARY INFORMATION

for

Classifying hydrogen-rich superconductors

E. F. Talantsev^{1,2}

¹M.N. Miheev Institute of Metal Physics, Ural Branch, Russian Academy of Sciences,
18, S. Kovalevskoy St., Ekaterinburg, 620108, Russia

²NANOTECH Centre, Ural Federal University, 19 Mira St., Ekaterinburg, 620002,
Russia

E-mail: evgeny.talantsev@imp.uran.ru

Supplementary Table I. $B_{c2}(T)$ dataset reported by Drozdov *et al.* [1] for “cooling” stage of LaH₁₀ subjected to pressure of $P = 150$ GPa. Values were deduced by 50% of normal state resistance criterion from Fig. 2(a) [1].

T (K)	B_{c2} (T)
241.68	0
241.68	0
241.53	0.2
241.26	0.5
239.41	2
236.86	3
236.91	3
233.23	6
229.99	9

Supplementary Table II. $B_{c2}(T)$ dataset reported by Drozdov *et al.* [1] for “warming” stage of LaH₁₀ subjected to pressure of $P = 150$ GPa. Values were deduced by 50% of normal state resistance criterion from Fig. 2(a) [1].

T (K)	B_{c2} (T)
245.1	0
242.5	3
239.0	6
235.7	9

Reference

[1] Drozdov A P, *et al* 2019 Superconductivity at 250 K in lanthanum hydride under high pressures *Nature* **569** 528-531